World Conference on Timber Engineering Oslo 2023

STRUCTURAL PERFORMANCE OF TWO-PANEL CLT SHEAR WALL WITH BOLTED CONNECTION

Daiki Hinata[1], Jun Kubota[2], Takashi Shima[3], Shinji Takatani[4], Masanori Hisada[5], Naohiro Haneda[6]

ABSTRACT: The increasing demand for using timber structures as building structures has led to the development of many cross-laminated timber (CLT) shear wall systems including details on connecting the walls. However, these details are still not sufficient for quick and easy installation purposes. Therefore, ways of improving the installation productivity on site are required. In this study, we propose installing a pair of CLT panels as a single shear wall, i.e., a two-panel CLT shear wall, with bolted connections as a solution. The heavier CLT panels are, the more difficult on-site installation work becomes. If the panels are divided into two, they would be easier to handle as each panel is lighter. Furthermore, a bolted connection is one of the easiest on-site installation connections. This paper presents the structural performances of a two-panel integrated CLT shear wall with bolted connection, which was investigated in element tests on bolted connections and full-scale wall tests. An FE analysis was also conducted to investigate the stresses on the CLT panels and the ultimate behaviors. The results indicated that this system has a high lateral resisting strength and ductility.

KEYWORDS: CLT shear wall, Two-panel CLT wall, Structural test and FE analysis, High productivity

1 INTRODUCTION

The demand for timber components for building structures has been increasing around the world, leading to the development of many cross-laminated timber (CLT) shear wall systems which include connection details [1-3]. However, the connections for CLT shear walls are difficult to install quickly and efficiently. When installing CLT shear wall panels in a steel moment-resisting frame, steel plates are typically inserted into the CLT panel with a slit at the top and bottom, integrating it by driving in drift pins, and bolting the inserted steel plate to a gusset plate pre-installed on a column or beam [3]. This method has two connections between the CLT panel and steel frame, CLT panel-to-steel plate and steel plate-to-gusset plate, which causes low productivity of construction due to the work for installing both connections. Moreover, drift pin connections must be fabricated extremely precisely because the bores for drift pins need to match that on the steel plates, due to the minimum tolerance requirement. It is crucial to find ways of improving installation efficiency on site. Thus, we propose installing a pair of CLT panels as a single shear wall, i.e., a two-panel CLT shear wall, with a bolted connection as a solution. Figure 1 shows sketches of this system in which two sheets of CLT panels are installed on both sides of the gusset plates. The heavier CLT panels are, the more difficult on-site installation work becomes. If the CLT panels are divided into two panels, they can be easier to handle because each panel is lighter. In addition, a bolted connection is one of the easiest to install on site. This paper presents the structural performance of the two-panel integrated CLT shear wall with the bolted connection, which is investigated through element tests for the bolted connections and full-scale wall tests. We also conduct an FE analysis to investigate the stresses in the CLT panels and ultimate behaviors.

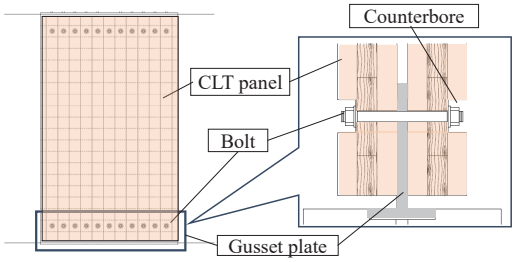

Figure 1: *Sketches of two-panel CLT shear wall*

2 ELEMENT TEST FOR BOLTED CONNECTION

2.1 TEST OVERVIEW

To verify the structural performances of the developed two-panel CLT shear walls with bolted connections and

[1] Daiki Hinata, Kajima Technical Research Institute, Kajima corporation, Japan, hinata@kajima.com
[2] Jun Kubota, Kajima Technical Research Institute, Kajima corporation, Japan, jkubota@kajima.com
[3] Takashi Shima, Kajima Technical Research Institute, Kajima corporation, Japan, shimata@kajima.com
[4] Shinji Takatani, Architectural Design Division, Kajima corporation, Japan, takatani@kajima.com
[5] Masanori Hisada, Architectural Design Division, Kajima corporation, Japan, hisadam@kajima.com
[6] Naohiro Haneda, Architectural Design Division, Kajima corporation, Japan, haneda@kajima.com

https://doi.org/10.52202/069179-0375

determine an appropriate bolt configuration on the CLT shear wall, we conducted element tests for the bolted connections. The tested connections consist of steel plates, assumed to be gusset plates, a pair of CLT panel pieces, and bolts. The bolted connections are shown in Table 1 and Figure 2. In this study, seven types of bolted connections were tested. The parameters were the grade and lamina composition of the CLT, the loading direction of the CLT, and the bolt diameter and arrangement. We used S60 grade 3-ply 3-layer CLTs with a lamina width of 120 mm and thickness of 90 mm, without edge bonding, and S60 grade 5-ply 5-layer CLTs with a lamina width of 122 mm and thickness of 150 mm, with edge bonding. We also conducted tests on M20 series connections with two rows of bolts in the major direction.

It was previously found that the placement of the bending connections, such as drift pins and bolts, between the laminae on the CLT panel can degrade shear strength [4]. Therefore, to eliminate these effects, bolted connections were placed at the center of the lamina width for the CLT shear wall in our study. Accordingly, the CLT panel width of the test area on the element tests is the same as that of the single lamina. Although the structural performance of the bolted joints has been shown to be sufficient in previous experimental results [5], in our study, the CLT panel includes counterbores to prevent the bolt heads from protruding from the face of the CLT panels, for the sake of visibility.

The tests were carried out by applying a tensile force to the upper and lower steel plates attached to the connection, using a universal testing machine. The relative displacements between the steel plate at the position of bolted connections and CLT panels at the same level were measured by LVDTs. We used average relative displacements of the right and left for the following evaluations.

2.2 TEST RESULTS

The relationship between force and displacement is shown in Figure 3, the representative failure mode in Figure 4, and the ultimate strength and initial stiffness derived based on perfect elasto-plastic modeling [6] in Table 2. The bolted connection is not expected to deform more than 40 mm in the CLT shear wall connections because this only occurs when the CLT shear wall drift angle is over 1/20 radians. Therefore, only element test data up to a displacement of 40 mm were used for the evaluation. In Figure 3, the force-displacement curves were shifted to eliminate the influence of the initial slip, which is within approximately 1.5 mm, due to the bolt-hole clearance according to the perfect elasto-plastic modeling rule [6] so that the straight lines between 0.1 Pmax and 0.4 Pmax match zero force / zero displacement point.

At the beginning of all tests, the strength increased almost linearly; however, the slope of the force-displacement curve decreased due to the pop-out failure at the inner lamina (the side in contact with the steel plate) with the width of the bolt diameter in the major direction loading tests, as well as split failure of the inner orthogonal lamina in the minor direction loading tests. The strength was still maintained, mainly due to the resistance of the outer lamina. As the deformation increased, the bolt heads and washers appeared to be significantly embedded in the CLT. After the tests, we observed that all bolts were bent at the center.

The M12 series demonstrated stable structural behavior, regardless of the loading direction, and no significant decrease in strength was observed. Because the M20 series contained thicker CLT panels (5-layer and 5-ply), the major direction tests showed stable structural performance up to a displacement of 40 mm even in the connection with two rows of bolts. However, in the minor

Table 1: *Details and parameters of bolted connection element tests*

ID	Bolt				CLT				Number of tests
	Diameter [mm]	Yield Point [N/mm^2]	Number @Pitch	Bore Dia. [mm]	Grade Layer-ply	Thickness [mm]	Counterbore Dia × Depth [mm]	Direction	
90-M12S	12	400	1	13	S60-3-3	2×90	φ 36×29	Major	6
90-M12W								Minor	6
90-M16S	16	400	1	17	S60-3-3	2×90	φ 50×29	Major	6
90-M16W								Minor	6
150-M20S	20	490	1	21	S60-5-5	2×150	φ 55×50	Major	6
150-M20W								Minor	6
150-2xM20S			2-@120					Major	6

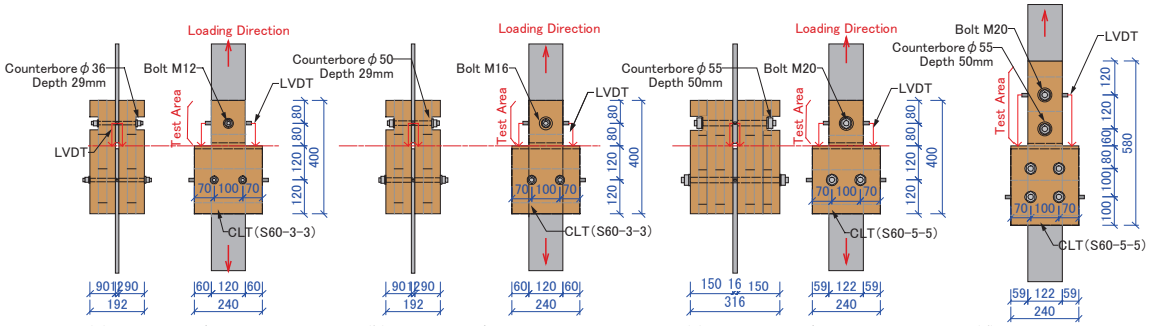

(a) 90-M12S / W *(b) 90-M16S / W* *(c) 150-M20S / W* *(d) 150-2xM20S*

Figure 2: *Configuration of bolted connection element tests*

https://doi.org/10.52202/069179-0375

direction tests, damage to the laminae led to ultimate failure when the deformation was approximately 5 mm. For the six specimens in all tests, the behaviors were approximately similar.

The ultimate strength and initial stiffness tend to be larger for larger bolt diameters and connections arranged in the major direction. Although the strength of the two rows of bolts connection was expected to be less than twice the strength of a single bolt connection due to the group effect, within the scope of this test, the connections with two rows of bolts had approximately the same failure mode as that of the single bolt type, and its strength was slightly higher than that of the single bolt ones.

Thus, we verified that this bolted connection with CLT placed in the major direction is sufficiently ductile with little decrease in strength even after exceeding the elastic limit. Meanwhile, the minor direction connections demonstrated fewer deformation capacities compared with the major direction specimens, indicating that providing a sufficient margin for the bolt connection strength in the CLT minor direction of the shear wall is important for the structural design.

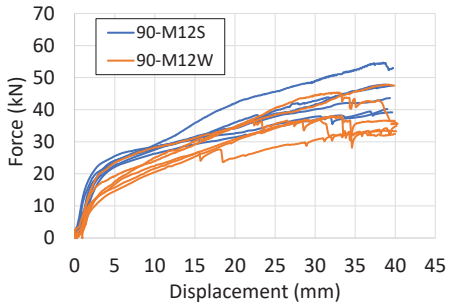

(a) Bolt M12 series

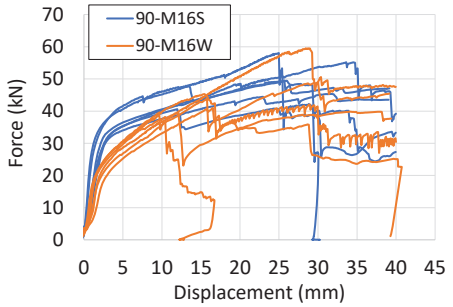

(b) Bolt M16 series

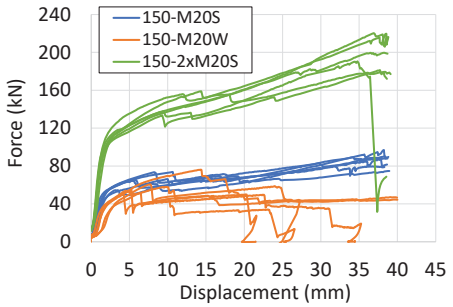

(c) Bolt M20 series

Figure 3: *Relationship between tensile force and average displacement in bolted connection element tests*

Table 2: *Ultimate strength and initial stiffness from bolted connection element tests*

ID	Mean Ultimate Strength [kN]	Mean Initial Stiffness [kN/mm]
90-M12S	36.9	5.2
90-M12W	32.1	3.3
90-M16S	44.0	13.4
90-M16W	38.3	8.8
150-M20S	71.3	17.5
150-M20W	51.2	17.7
150-2xM20S	160.7	37.9

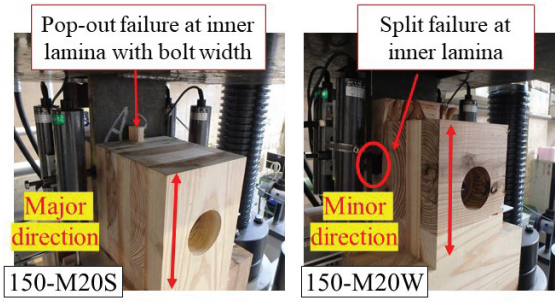

Figure 4: *Representative failure mode*

3 FULL-SCALE CLT SHEAR WALL TEST AND ANALYSIS

3.1 STRUCTURAL TEST OUTLINE

A list of full-scale two-panel CLT shear walls is shown in Table 3, the diagrams are shown in Figure 5, and photos of the test setup are shown in Figure 6. The CLT test walls consist of a gusset plate attached to a steel stub, a pair of CLT panels, and bolts. The parameters were the vertical and horizontal dimensions, CLT composition, and bolt configuration. The combination of bolt diameter and CLT compositions in the CLT wall are the same as the element test detail, and as with the element specimens, bolts were arranged at the center of each CLT lamina width. A clearance of 40 mm was provided between the CLT edge and the upper and lower steel stubs to avoid generating friction forces and compression struts when deformation increased. During the tests, lateral forces were applied to the top of the specimens, and the vertical jacks kept the steel stubs horizontal while allowing them to move vertically. The loading protocol was as follows: ±1/600, ±1/450, ±1/300, ±1/200, ±1/150, ±1/100, ±1/75, and ±1/50 radians for three cycles and ±1/30 and ±1/20 radians for two cycles.

In the S-M12 and S-M16 tests, no damage to the CLT panels was observed while the loading. In the S-M20, a failure of the inner lamina near the outermost bolt was observed at the -1/20 radians peak, as in the element tests. M-M20, with two rows of bolts, also showed no strength reduction, although there were two pop-out failures at the edge of the CLT panels at 1/50 radians and three at 1/20 radians due to bolt deformation. The reason the CLT panels were not damaged was that the average shear stress of the CLT panels at ultimate strength was about 0.66 N/mm^2, which was less than the standard shear failure stress of CLT panels. The strength and initial stiffness of

https://doi.org/10.52202/069179-0375

Table 3: *Dimensions and parameters of full-scale CLT shear walls*

ID	Dimension		Bolt				CLT		
	W [mm]	H [mm]	Dia.	Yield Point [N/mm^2]	Configuration Row-Number	Bore Dia. [mm]	Grade Layers	Thickness [mm]	Counterbore Dia × Depth [mm]
S-M12	1440	2400	M12	400	1-11	13	2x S60-3-3	2×90	φ36×20
S-M16	1440	2400	M16	400	1-11	17	2x S60-3-3	2×90	φ50×27
S-M20	1220	3150	M20	490	1-9	21	2x S60-5-5	2×150	φ55×50
M-M20	1220	3150	M20	490	2-9	21	2x S60-5-5	2×150	φ55×50

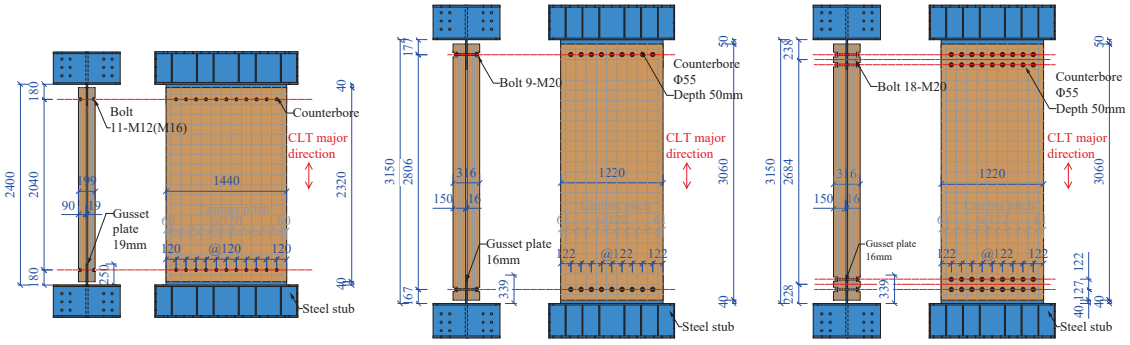

(a) S-M12(M16) *(b) S-M20* *(c) M-M20*

Figure 5: *Configuration of full-scale CLT shear walls*

M-M20 with two rows of M20 bolts tended to be slightly higher than twice the strength of S-M20.

After the test, the CLT walls were decomposed to determine the internal damage on the CLT panels. The inside of the CLT panel of S-M16 is shown in Figure 7. We observed bolt tracks in the diagonal direction with a length of 40 mm in total in the outermost position, as well as bent bolts.

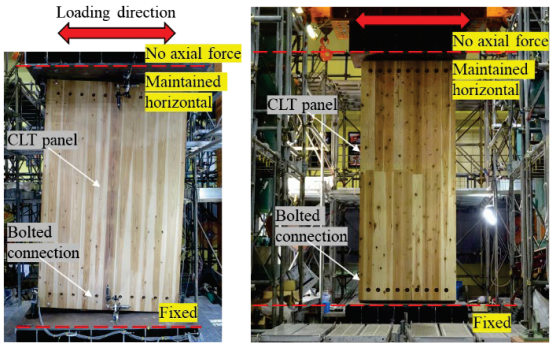

(a) S-M12 *(b) S-M20*

Figure 6: *Full-scale CLT shear wall test setup*

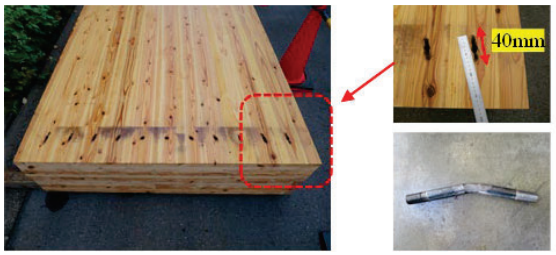

Figure 7: *Inside of S-M16 CLT panel (left: back side of CLT panel, top right: bolt track, bottom right: bent bolt)*

3.2 SIMULATION ANALYSIS OUTLINE

To establish an analysis method for this two-panel CLT shear wall, we compared the test results with the simulation results obtained from an FE analysis. In addition, we also investigate the stress states of the CLT shear walls. The analysis was performed using the MSC Nastran 2019.0 software with monotonic loading. In the analytical model, the gusset plates and CLT panels were modeled with elastic shell elements, and the bolted connection was modeled with nonlinear spring elements in two directions (vertical and horizontal) connecting the gusset plates and CLT panels. Elastic orthogonal anisotropy was applied to the shell elements of the CLT panels as material properties, and the elastic moduli in the major direction, minor direction, and shear were determined by the values of standard [7]. The nonlinear characteristics of the spring elements were assumed to be perfect elasto-plastic. The yielding point and initial stiffness were calculated from the element test results of the major and minor CLT panel directions by using Hankinson's equation shown in equation (1). An outline of the calculation methods is shown in Figure 8. The ultimate strength (P0, P90) and initial stiffness (K0, K90) from the CLT element tests on the major and minor directions are inserted into Hankinson's equation, and the characteristic values (Pθ, Kθ) in the θ direction are then separated into vertical and horizontal components (Pθ_0, Pθ_90, Kθ_0, Kθ_90) by applying a trigonometric function. However, it is necessary to determine the deformation angles of each connection, as observed in the tested CLT wall, because the structural properties depend on the loading direction in practice. Thus, a convergence calculation was used to obtain the deformation angle θ. As shown in the procedure in Figure 9, the deformation angle θ was calculated so that all CLT panel elements and the

https://doi.org/10.52202/069179-0375

springs of bolted connections are satisfied with equilibrium of the deformation and stress.

$$P_\theta = \frac{P_0 \cdot P_{90}}{P_0 \cdot \sin^2\theta + P_{90} \cdot \cos^2\theta} \quad (1)$$

Where P_θ=strength in the θ direction, θ=deformation angle. This equation can be used for stiffness K instead of strength P.

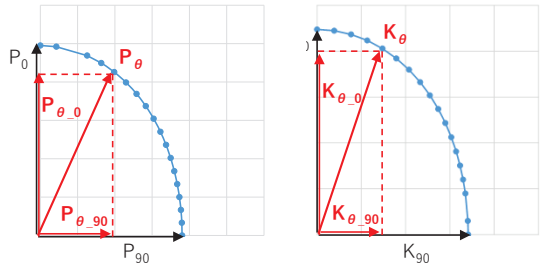

Figure 8: *Calculation method for spring properties at a specific angle*

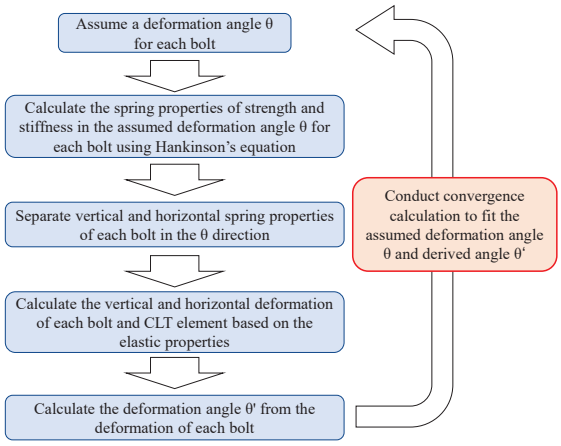

Figure 9*: Convergence calculation process*

3.3 DISCUSSION OF TEST AND ANALYSIS RESULTS

The ultimate strength and initial stiffness calculated by perfect elasto-plastic modeling are listed in Table 4, and Figure 10 shows the relationship between shear force and drift, and its skeleton curves from the full-scale CLT wall tests and simulation. The drift angle on hysteresis curves was calculated by dividing the horizontal displacement between the top and bottom steel stubs by the height between them.

In all specimens, the strength continued to increase up to 1/20 radians, and no significant reduction in strength was observed, indicating that the CLT shear wall exhibited a substantially high deformation capacity. Furthermore, a clearance of +1 mm at the bores on the CLT panel and gusset plates for the bolted connection did not cause slip behavior throughout the tests.

The shear force-drift relationship from the simulation for each CLT shear wall is largely consistent with the test skeleton curves. Because the yielding point of the outermost bolts in the analysis coincides with the elastic limit on the tests, we conclude that the specimens reached the maximum strength through a gradual reduction in stiffness due to the yielding of the bolts. Moreover, from the above, it can be said that the bolt strengths in the analysis were set at a reasonable value. In the S-M16, S-M20, and M-M20 tests, the initial stiffness in the test and the analysis were almost identical. However, in the S-M12 test, the initial stiffness of the analysis was lower than in the test results. One reason for this may be that the initial stiffness obtained by the perfect elasto-plastic modeling of the element tests for the M12 series was evaluated to be lower than the actual values. In the modeling, the initial stiffness is calculated based on the slope connecting the points at 0.1 Pmax and 0.4 Pmax. The evaluation of the test result with the M12 bolt seemed to be affected when the stiffness had already decreased at the 0.4 Pmax point because the maximum strength is much higher than the elastic limit. As a result, it is possible to estimate the initial stiffness of this CLT shear wall from the element test results, but it also illustrates the importance of using the appropriate initial stiffness for the connection.

Hankinson's equation used to calculate the stiffness and strength at an angle was originally devised for materials with a constant wood grain direction, such as lumber and glued laminated wood, and is not intended to be applied to composite materials with orthogonal wood grain directions in each layer, such as CLT. However, we found that the bolted connection showed similar behavior to that of glued laminated timber as the laminae located close to the gusset plate mainly resisted the bolt deformation. This suggests that Hankinson's equation can be used to estimate the spring properties at a specific angle in the bolted connection.

Figure 11 shows the vertical and shear strain contour and the maximum and minimum strain at +1/20 radians for the S-M16 and M-M20 FE analyses, which contain larger values in the same dimension of the CLT shear wall. The shear strain contour indicates that the strain is concentrated at the center of the CLT panel, and the maximum strain in M-M20 at a large deformation is over 3500 μ, which is beyond an allowable value. However, the strain in the surrounding area was kept small, which is consistent with the full-scale test results that showed no damage to the CLT panels.

In conclusion, although there are some issues in the evaluation of stiffness, this simulation method can be used to evaluate the structural performance of the CLT shear wall with sufficient practical accuracy.

Table 4: *Ultimate strength and initial stiffness of CLT shear walls*

ID	Ultimate Strength [kN]		Stress		Initial Stiffness [kN/×10^{-3}rad]	
			Flexural [N/mm^2]	Shear [N/mm^2]		
	Positive	Negative	Absolute mean	Absolute mean	Positive	Negative
S-M12	97.8	-88.6	1.53	0.36	9.0	8.8
S-M16	132.3	-128.5	2.14	0.50	14.4	14.9
S-M20	114.4	-110.2	2.12	0.31	8.7	9.2
M-M20	249.6	-235.5	4.67	0.66	18.4	18.2

https://doi.org/10.52202/069179-0375

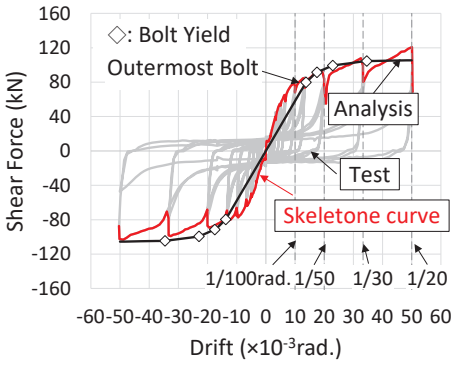

(a) S-M12

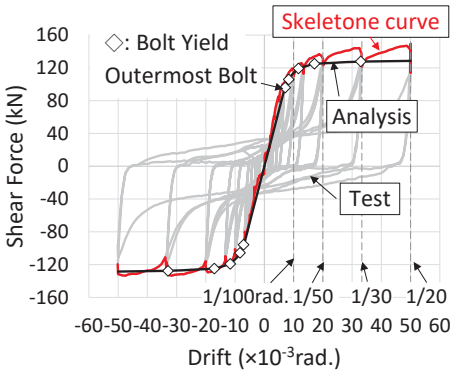

(b) S-M16

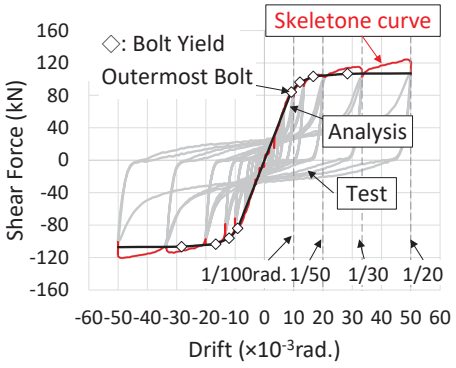

(c) S-M20

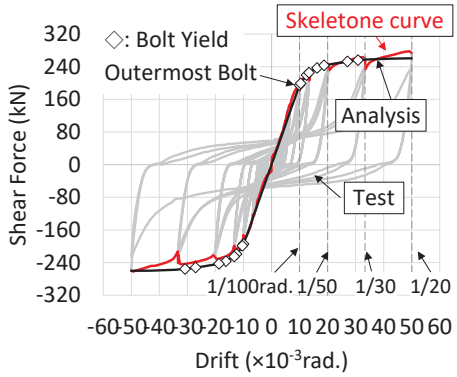

(d) M-M20

Figure 10: *Relationship between lateral shear force and drift angle from test and analysis results of CLT shear wall*

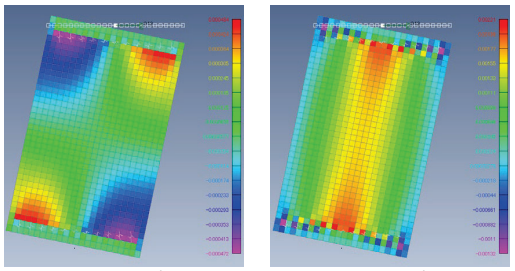

(a) S-M16

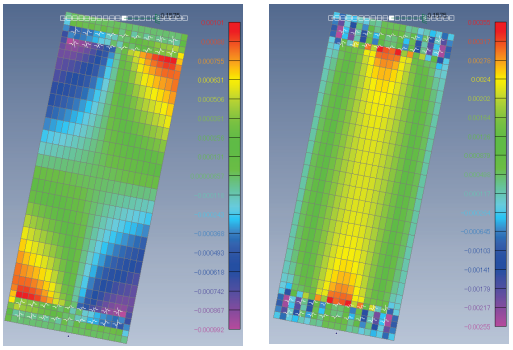

(b) M-M20

Figure 11: *Strain contour of CLT panel obtained by FE analysis at 1/20 radians (right: Vertical strain, left: Shear strain)*

4 CONCLUSION

To improve on-site productivity, we have developed a two-panel CLT shear wall system with a novel bolted connection in which a steel plate is sandwiched between a pair of CLT panels. In the study, we conducted element tests on the bolted connection, a full-scale shear wall test, and an FE analysis. The results showed that this system has a high lateral resisting strength and ductility. Our findings are summarized as follows.

The bolted connections showed high deformation capacities even beyond the elastic limit when the force was subjected to the CLT major direction within the range of the tests.

The full-scale CLT shear wall tests showed that the CLT panels were not damaged up to a large deformation of 1/20 radians in all specimens and the CLT panels had high deformation capacity with no reduction in strength.

For the FE analysis, Hankinson's equation was applied to the element test results to estimate the spring properties of the bolted connection. The simulation results showed that the analytical results were highly consistent with the test results, except for some initial stiffness. Thus, we can conclude that the analytical method is feasible for simulating the structural behaviors of the two-panel CLT shear wall.

REFERENCES

[1] E. J. Baas, G. Granello, A. R. Barbosa, M. Riggio, Post-Tensioned Timber Wall Buildings: Design & Construction Practice in New Zealand & United

https://doi.org/10.52202/069179-0375

States. World Conference on Timber Engineering 2020, Santiago, 2021.
[2] M. Popovski, Z. Chen, A. Iqbal, Performance of Post-Tensioned CLT Shear Walls with Energy Dissipators under Lateral Loads. World Conference on Timber Engineering 2020, Santiago, 2021.
[3] K. Kanazawa: Structural Performance of Composite Structure with CLT Infilled in Steel Frames Using Joint of Drift-pin with Steel Plate. Summaries of Technical Papers of Annual Meeting Architectural Institute of Japan, C-2, Structures IV, pp. 331-334, 2019.9. (in Japanese)
[4] K. Nakatsuji, H. Yamazaki, H. Sakata, N. Toba, Y. Nonaka, A Study on Shear Performance of CLT Connection Using Drift Pins and Insert-steel Gusset Plate, J. Struct. Constr. Eng., AIJ, Vol. 83 No. 754, pp. 1811-1820, Dec. 2018 (in Japanese)
[5] J. Kubota, D. Hinata, Y. Tanaka, S. Takatani, N. Haneda, Evaluation of Structural Properties of Bolt Joint between CLT and Steel Plate. Summaries of Technical Papers of Annual Meeting Architectural Institute of Japan, C-2, Structures IV, pp. 311-312, 2021.9. (in Japanese)
[6] Architectural Institute of Japan: AIJ Standard for Structural Design of Timber Structures, Tokyo, Japan, Maruzen, 2006. (in Japanese)
[7] Japan Housing and Wood Technology Center: Design and construction manual on CLT building version 2016, Tokyo, Japan, 2016. (in Japanese)